Supporting Information

Addressing Serine Lability in a Paramagnetic Dimethyl Sulfoxide Reductase Catalytic Intermediate

Khadanand KC, Jing Yang, and Martin L. Kirk[*]

Department of Chemistry and Chemical Biology, The University of New Mexico, MSC03 2060, 1 University of New Mexico, Albuquerque, NM 87131-0001, USA

mkirk@unm.edu

Table of Contents

1. Synthesis of Compounds 1 and 2

Synthesis of [BTEA]$^+$[Mo(V)(dped)$_2$(^{t}CAT)]$^{1-}$ (1). <u>Solvent preparation</u>: Acetonitrile was first dried with powdered KOH and then filtered. The filtrate was distilled overnight in P_2O_5 under a N_2 atmosphere. THF and diethyl ether were distilled in Na/Benzophenone. All of these distilled solvents (CH_3CN, THF, and diethyl ether) were then stored over molecular sieves for three days.

For the synthesis of complex **1** (Scheme 1), 210 mg KBut^{t}O was dissolved in 10 ml THF. 100 mg of 3,5-di-tert-butylcatechol was dissolved in 10 ml THF. Both solutions were flushed with dry N_2 gas for 30 minutes, and then the catechol solution was transferred via canula into the KBut^{t}O solution that was pre-cooled to -10 $^{\circ}$C. The mixture was stirred for 15 minutes. The solution was then transferred to a 50 ml round bottom flask containing a partially dissolved solution of Mo(pdt)$_2$(CO)$_2$[1] (100 mg in 10 ml CH_3CN) flushed with N_2 at -10°C. The mixture was stirred for 15 minutes and then a benzyltriethylammonium chloride solution (70 mg in 10 ml CH_3CN) was added. The green colored solution persisted for a few hours and then changed to a reddish-purple color. The solution was left to continue stirring overnight and then the solution was dried by purging with N_2 gas. The resulting dried powder was re-dissolved in CH_3CN and filtered through Ceilite 545 under N_2 protection. The filtrate was transferred into a 100 ml flask containing about 30 ml ether, then additional ether was added to produce a precipitate. The supernatant liquid was removed through a canula with positive N_2 pressure. Recrystallization procedures were repeated twice, and the product was dried under vacuum for 3-4 hours. The yield was 70 mg (44.6%). The complex was then characterized by mass spectrometry (observed mass 802.0970 and theoretical mass 802.0965), EPR, and UV-Vis-NIR. The nature of the coordinating ligands to Mo were determined by EXAFS. Since the complex is highly unstable, a crystal structure determination was not successful. The elemental analysis for this complex was also unsuccessful due to the highly unstable nature of this enzyme intermediate analog.

Synthesis of [BTEA]$^+$[Mo$^{(V)}$(cydt)$_2$(^{t}CAT)]$^{1-}$ (2). The synthetic (Scheme 1) and characterization methods for complex **2** were similar to that for complex **1**. To synthesize this complex, 35 mg of KBut^{t}O (in 6 ml THF) was treated with 30 mg of 3,5-di-tert-butylcatechol (in 5ml THF). The acid-base mixture was added to 30 mg of Mo(cydt)$_2$(CO)$_2$[2] (6 ml acetonitrile) dissolved in acetonitrile. 30 mg of benzyltriethylammonium chloride in 5 ml acetonitrile was then added to the mixture. The blue color persisted for few hours and upon stirring overnight the color changed to purple. After two recrystallizations, the yield was 25mg (46%). The complex was characterized by mass spectrometry (observed mass 606.0673 and theoretical mass 606.0652), EPR, and UV-Vis-NIR. The nature of the coordinating ligands to Mo were determined by EXAFS. The complex is highly unstable (albeit, more stable compared to complex **1**) and we
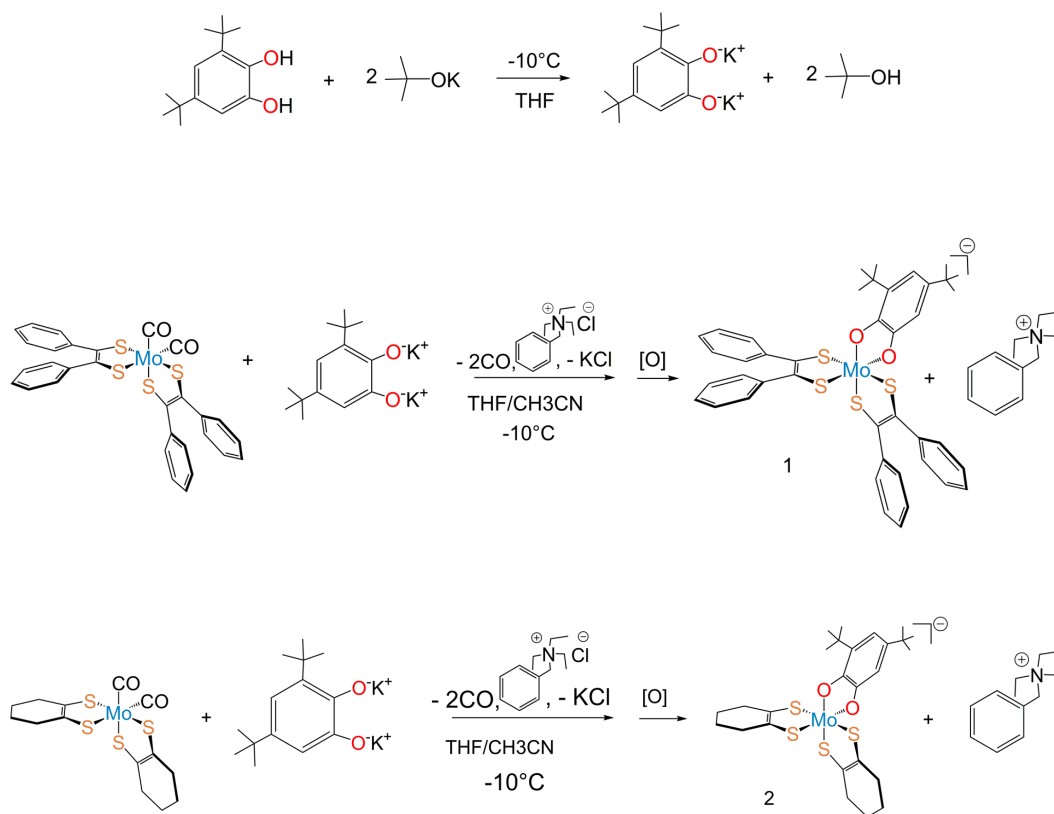
Scheme S1: Synthesis of models **1** and **2**

were not able to obtain a crystal suitable for X-ray diffraction. The elemental analysis for this complex was also unsuccessful due to the highly unstable nature of this enzyme intermediate analog.

2. Computational

Spin unrestricted geometry optimizations were performed at the density functional theory (DFT) level using the hybrid exchange-correlation functional (B3LYP). Computations were performed using the ORCA suite (v 4.0.0).[3-5] Computations of models **1** and **2** used valence triple-zeta polarization (TZVP) basis sets for all elements. Computational models C-E used the TZVP basis set for Mo and S and a valence double-zeta (SVP) basis set was used for the other elements. EPR spin-Hamiltonian calculations employed the zeroth order relativistic approximation (ZORA) Hamiltonian for the relativistic correction and the old-ZORA-TZVP basis set for Mo and the ZORA-def2-TZVP(SVP) basis set for other elements.

Computational model **A** is derived from the fully optimized 6-coordinate complex **1**, but with one of the catechol oxygens replaced by a hydrogen atom. The 5-coordinate model **B** and 6-coordinate models **C** and **D** are fully geometry optimized structures. The 5-coordinate model **E** possesses the same dithiolene dihedral angle as is found in the crystal structure of DMSOR (1EU1).[6]
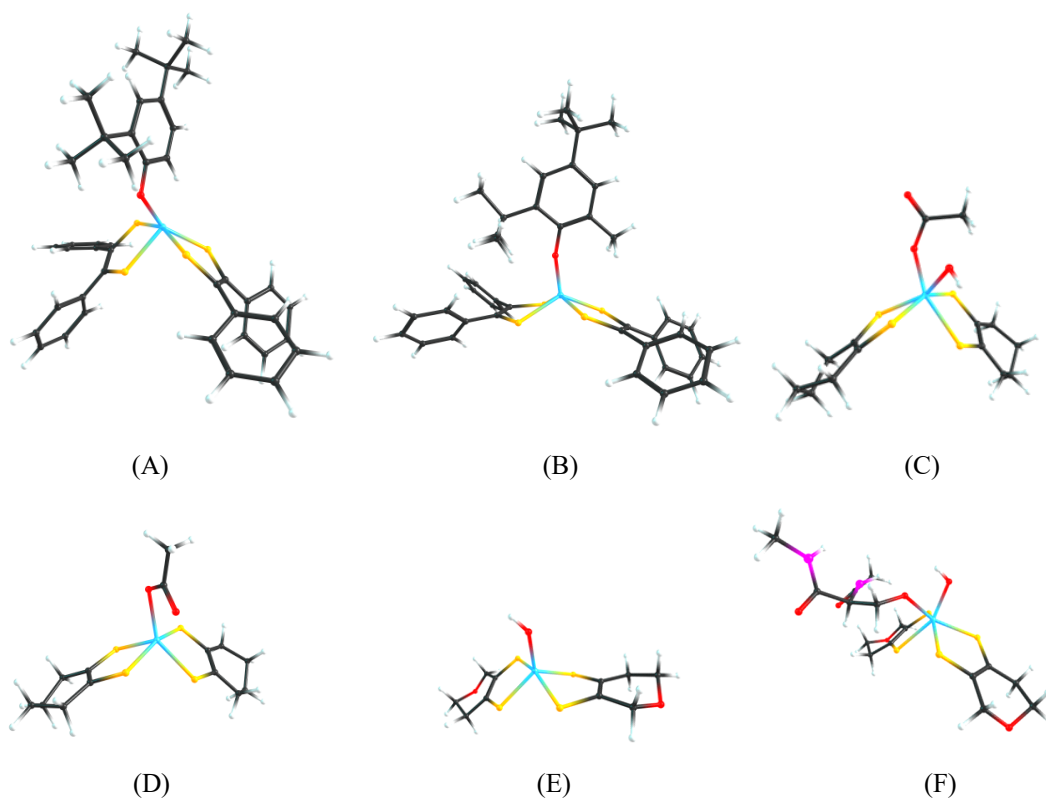

(A) (B) (C)

(D) (E) (F)

Figure S1: (**A**) [Mo(dped)$_2$(2,4-*di-tert*-butylphenolate)]$^{1-}$ (structure from **1**), (**B**) [Mo(dped)$_2$(2,4-*di-tert*-butyl-2-methylphenolate)]$^{1-}$, (**C**) [Mo(cydt)$_2$(Ac)(OH)]$^{1-}$, (**D**) [Mo(cydt)$_2$(Ac)]$^{1-}$, (**E**) [Mo(prdt)$_2$(OH)], (**F**) [Mo(V)(prdt)$_2$(SerO)(OH)]^1 (the dihedral angle and two carbons in protein backbone are taken from the structure of oxidized DMSOR (PDB-1EU1).

3. EPR Spectroscopy

Table S1. EPR spin-Hamiltonian parameters for Nar/DMSOr and Models

Computational Models	g_1	g_2	g_3	$g_{ave}(g_{iso})$
(A)	2.0029	1.9702	1.8943	1.9558
(B)	2.0350	1.9934	1.9672	1.9986
(C)	2.0300	1.9796	1.9404	1.9833
(D)	1.9855	1.9786	1.9455	1.9698
(E)	2.0273	1.9830	1.9554	1.9886
(F)	2.0076	1.9836	1.9626	1.9846

Experimental and Data Analysis: EPR data were collected at X-band using a Bruker EMX spectrometer with associated Bruker magnet control electronics and microwave bridges. The microwave frequency was ~9.39 GHz (for complexes **1** and **2** at RT/77K the microwave frequencies were 9.3881/9.3970 GHz and 9.3873/9.4102 GHz, respectively). The modulation amplitude was set at 1mT and the frequency modulation was adjusted to 20 MHz for complex **1** and 100 MHz for complex **2** at low temperature. At room temperature, the frequency modulation was fixed at 100 MHz for both complexes. The field attenuation was set at 30 dB. The Mo(V) EPR resonance field was observed at ~330 mT. Compounds **1** and **2** were dissolved in n-butyronitrile (BN) for low temperature studies and [acetonitrile for the room temperature EPR experiments. These solutions were subsequently transferred under positive nitrogen pressure via canula to N_2 purged dry EPR tubes. EPR simulations were performed using the MATLAB toolbox and the EasySpin suite (v5.2.28).[7]

Table S2. EPR spin-Hamiltonian parameters for DMSOr and Models

DMSOr/ Models	g-tensor				^{95,97}Mo A-tensor ($\times 10^{-4}$ cm^{-1})[d]				Euler angles (deg)
	g_1	g_2	g_3	g_{ave} (g_{iso})	A_1	A_2	A_3	A_{ave} (A_{iso})	α, β, γ
NarGHI lpH[a]	2.0009	1.9847	1.9638	1.9831	na	na	na	na	na
NarGHI hpH[a]	1.9869	1.9800	1.9638	1.9607	na	na	na	na	na
DMSOr[b]	1.9988	1.9885	1.9722	1.9865	17.78	-20.89	3.11	34.22	14.3, 85.9, 5.7
1[c]	2.0066	1.9881	1.9655	1.9867 (1.9843)	16.38	-17.76	1.39	32.28 (31.69)	-0.9, 58.2, 3.3
2[c]	2.0110	1.9856	1.9636	1.9867 (1.9836)	13.54	-22.29	9.08	33.62 (33.02)	3.7, 75.6, 1.0
1 *(cal)*	2.0028	1.9889	1.9602	1.9840	15.98	-18.00	3.02	38.62	-5.8, 67.3, 2.2
2 *(cal)*	2.0121	1.9869	1.9639	1.9877	11.25	-20.65	9.51	41.07	5.8, 67.0, -2.3

Model compounds used in this study are labelled 1-2. [a]Ref. [b]DMSOR *high-g split* values Ref. [c]This work. [d]Dipolar contribution to the ^{95,97}Mo hyperfine tensor. Euler angles are defined as $R(\alpha,\beta,\gamma) = R_z(\alpha)R_y(\beta)R_z(\gamma)$. Anisotropic g-strain values ($\sigma_{1,2,3}$) in g units for 1 are 14.3x10^{-3}, 0.0x10^{-3}, and 13.4x10^{-3}, and for 2 are 2.3x10^{-3}, 0.1x10^{-3}, and 17.4x10^{-3}.

4. Spin Density Distributions and HOMOs

Spin Density of **1**   Spin Density of **2**

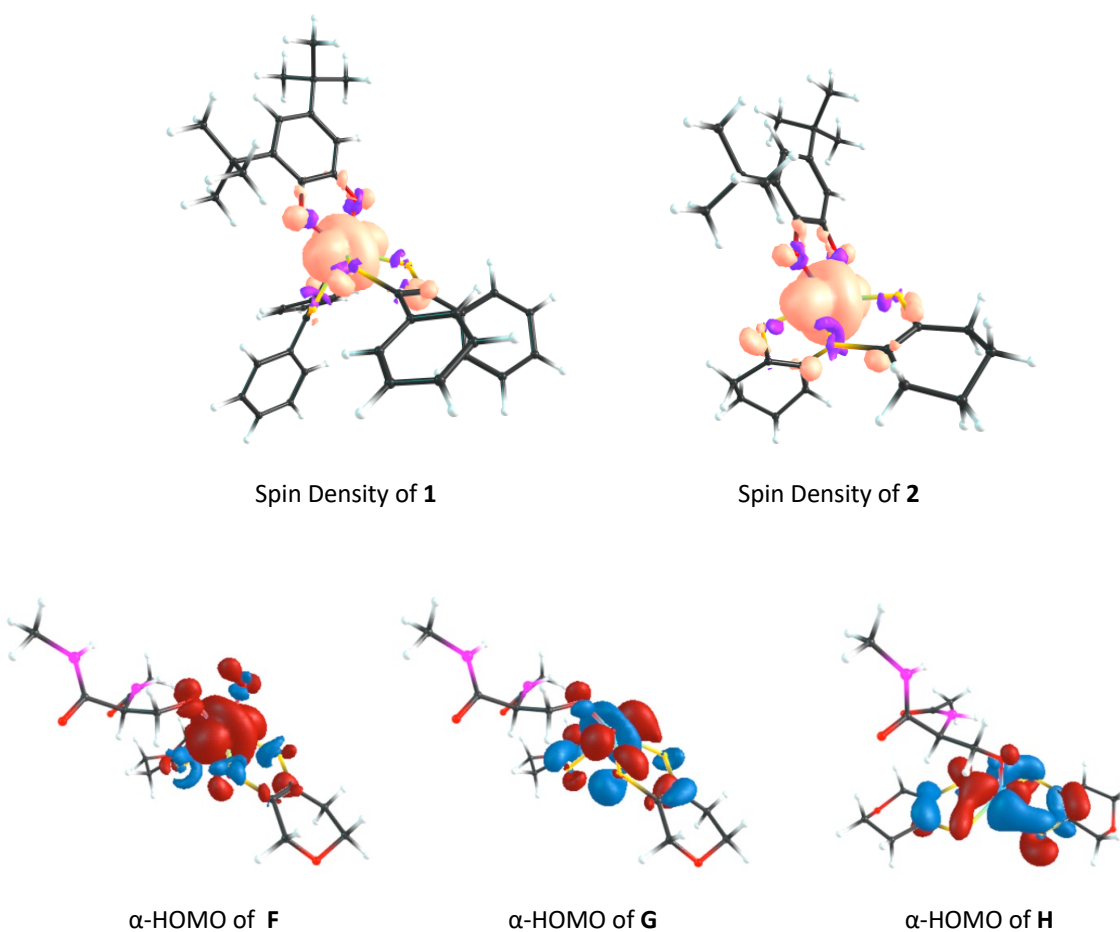α-HOMO of **F**   α-HOMO of **G**   α-HOMO of **H**

Figure S2: Top: Computed spin density distributions. Here, pale orange represents the positive spin density and purple the negative spin density. Bottom: The highest occupied molecular orbitals (HOMOs) of the computational models. *Note:* The structure of **G** was derived from **F** in Figure S1, and the structure of **H** is a fully optimized [Mo((IV)(prdt)$_2$(SerO)]$^{1-}$ structure. *Prdt* = 3,6-dihydro-2H-pyran-4,5-dithiolate.

5. EXAFS

Mo K-edge X-ray absorption spectroscopic data was collected on beamline 7-3 at the Stanford Synchrotron Radiation Lightsource (SSRL) with the SPEAR storage ring containing 200 – 300 mA at 3.0 GeV. Beamline 7-3 is equipped with rhodium-coated mirrors upstream and downstream of the Si (220) double-crystal monochromator. The incident and transmitted X-ray intensities (I_0, I_1, and I_2) were monitored with three nitrogen-filled ionization chambers. The sample temperature was maintained at 10 K using an Oxford Instruments CF1208 continuous flow liquid helium cryostat. Sample was prepared using 4 mg of **1** and **2** that were finely ground with 36 mg of BN powder. The samples was subsequently sealed in sample holders with sulfur-free Kapton tape. Data were collected in florescence mode (Mo Kα) using a Lytle detector. A Zr-3 filter and a Soller slit were used before the detector to reject the scattered radiation. The internal energy was calibrated using a Mo foil reference with the first inflection point set to 20,000 eV. XAS data were processed using the Demeter software suite (version 0.9.26).[8] The XANES spectra was calibrated and normalized in Athena[8] with the threshold energy assigned as 20,010 eV. The spectrum showing here is four-sweep averaged spectrum. The EXAFS simulations were performed using Artemis.[8] Backscattering paths were calculated from the embedded IFEFF (version IFEFF6) program using the DFT gas-phase optimized geometries for **1** and **2**.[8] All Fourier transforms were phase corrected using Mo-S backscattering. The data was fitted in k-space with the k range of 3.0 – 15.5 Å^{-1} for **1** and 3.4 – 15.4 Å^{-1} for **2**.
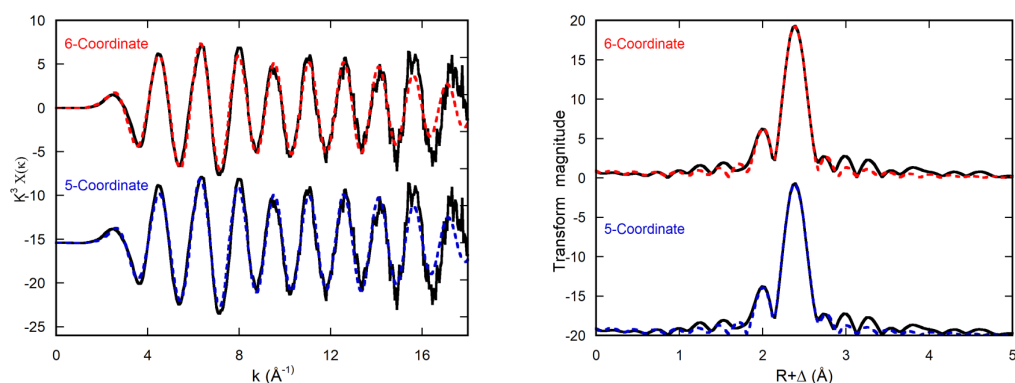

Figure S3: k-space data (left) and R-space daat (right) using fits 1 and 3. The k-space results for **1** used a k-range of 3-15.5 Å^{-1}.

Table S3: k-space fitting parameters for **1**

		Mo-S			Mo-O				
	N	R_{fit} (R_{guess})	σ^2	N	R_{fit} (R_{guess})	σ^2	S_o^2	ΔE_0	R_f (%)
Fit1	4	2.377(2.402)	0.0022	2	2.057(2.026)	0.0037	0.972	-0.36	3.46
Fit2	4	2.377(2.402)	0.0023	1	2.052(2.026)	0.0009	0.972	-0.16	3.49
Fit3	4	2.377(2.402)	0.0028	1	2.046(2.026)	0.0010	1.102	-1.67	3.05
Fit4	5	2.377(2.402)	0.0033	1	2.041(2.026)	0.0002	0.972	-1.98	3.24
Fit5	6	2.376(2.402)	0.0041	0			0.972	-1.33	9.17

Table S4: k-space fitting parameters for **2**

	Mo-S			Mo-O					
	N	R_{fit} (R_{guess})	σ^2	N	R_{fit} (R_{guess})	σ^2	S_o^2	ΔE_0	R_f (%)
Fit1	4	2.385(2.407)	0.0018	2	2.052(2.030)	0.0045	0.903	-1.912	5.11
Fit2	4	2.386(2.407)	0.0019	1	2.042(2.030)	0.0015	0.903	-1.10	4.01
Fit3	4	2.386(2.407)	0.0024	1	2.037(2.030)	0.0013	1.001	-1.382	4.13
Fit4	5	2.386(2.407)	0.0029	1	2.032(2.030)	0.0004	0.903	-1.366	4.69
Fit5	6	2.383(2.407)	0.0038	0			0.903	0.483	7.41

6. Orbital Compositions and Spin Populations for Models 1 and 2

Table S8: Fragment Orbital compositions (α-SOMO and β-LUMO) and Spin Populations for models **1** and **2**

		Molecular fragments						
				$S_{dithiolene}$		Cat	Dithiolene	
		Mo	Cat-*O,O*	P-pterin	Q-pterin		P-pterin	Q-pterin
(1) [Mo(dped)$_2$(CAT)]$^{1-}$	α-SOMO	37.6	5.9	17.9	8.3	7.6	33.5	16.0
	β-LUMO	59.4	4.0	5.7	8.9	5.9	14.1	16.2
	Spin population	+107.1	-2.2	-6.9	-5.4			
(2) [Mo(cydt)$_2$(CAT)]$^{1-}$	α-SOMO	42.6	5.9	14.5	15.9	8.2	22.1	24.6
	β-LUMO	66.4	3.6	8.7	7.9	5.7	13.1	12.0
	Spin population	+111.7	-6.7	-6.8	-3			

Spin populations are listed for atoms in italics. For $S_{dithiolene}$, the spin populations are the sum of those for both dithiolene sulfur atoms. Spin populations and fragment molecular orbital composition were calculated using Orca 4.0.0.

8. References

1.	Lim, B. S.; Donahue, J. P.; Holm, R. H., Synthesis and structures of bis(dithiolene)molybdenum complexes related to the active sites of the DMSO reductase enzyme family. *Inorg. Chem.* **2000,** *39* (2), 263-273.

2.	Sugimoto, H.; Harihara, M.; Shiro, M.; Sugimoto, K.; Tanaka, K.; Miyake, H.; Tsukube, H., Dioxo-molybdenum(VI) and mono-oxo-molybdenum(IV) complexes supported by new aliphatic dithiolene ligands: New models with weakened Mo=O bond characters for the arsenite oxidase active site. *Inorg. Chem.* **2005,** *44* (18), 6386-6392.

3.	Neese, F.; Wennmohs, F.; Hansen, A.; Becker, U., Efficient, approximate and parallel Hartree-Fock and hybrid DFT calculations. A 'chain-of-spheres' algorithm for the Hartree-Fock exchange. *Chem. Phys.* **2009,** *356* (1-3), 98-109.

4.	Neese, F., The ORCA program system. *Wiley Interdisciplinary Reviews: Computational Molecular Science* **2012,** *2* (1), 73-78.

5.	Neese, F., *ORCA, an Ab Initio, Density Functional, and Semi-Empirical Program Package, University of Bonn, Germany, 2012.*

6.	Li, H. L.; Temple, C.; Rajagopalan, K. V.; Schindelin, H., The 1.3 Å Crystal Structure of Rhodobacter sphaeroides Dimethyl Sulfoxide Reductase Reveals Two Distinct Molybdenum Coordination Environments. *J. Am. Chem. Soc.* **2000,** *122*, 7673.

7.	Stoll, S.; Schweiger, A., EasySpin, a comprehensive software package for spectral simulation and analysis in EPR. *J. Magn. Reson.* **2006,** *178*, 42.

8.	Ravel, B.; Newville, M., *ATHENA, ARTEMIS, HEPHAESTUS*: Data analysis for X-ray absorption spectroscopy using *IFEFFIT*. *Journal of Synchrotron Radiation* **2005,** *12*, 537-541.